Neuro
-endocrinology

Neuroendocrinology 1999;69:63–76

Received: May 12, 1998
Accepted after revision: September 16, 1998

# Projections of the Estrogen Receptor-Immunoreactive Ventrolateral Hypothalamus to Other Estrogen Receptor-Immunoreactive Sites in Female Guinea Pig Brain

Joanne C. Turcotte Jeffrey D. Blaustein

Neuroscience and Behavior Program, University of Massachusetts, Amherst, Mass., USA

**Key Words**
Periaqueductal gray · Sex behavior · Lordosis · Gonadal hormone receptors · Ventrolateral hypothalamus · Guinea pig

**Abstract**
The ventrolateral hypothalamus in female guinea pigs includes an estrogen receptor dense region adjacent to the ventromedial hypothalamus. This region is reciprocally connected with other estrogen receptor-containing areas suggesting that steroid hormone receptor-containing cells may be directly linked. *Phaseolus vulgaris* leucoagglutinin, an anterograde tract tracer, was specifically placed in this region with the aim of labeling some projections from estrogen receptor-containing neurons. These projections were colocalized immunocytochemically with the distribution of estrogen receptor-containing cells. Dense ventrolateral hypothalamic innervation was observed in some regions also containing a high concentration of estrogen receptor-containing cells. These regions included the medial preoptic area, the bed nucleus of the stria terminalis, the ventrolateral hypothalamus anterior and posterior to the injection site, and the midbrain central gray. A low density of ventrolateral hypothalamic fibers and terminals was observed in two regions rich in estrogen receptors, the amygdala and the arcuate nucleus. In general, ventrolateral hypothalamic fibers and terminals were present in all regions where estrogen receptors were found except the medial thalamus and habenular region. Labeled terminal boutons and perineuronal baskets were found around estrogen receptor-containing cells in most regions which contained estrogen receptor-containing cells. These close appositions were suggestive of synaptic contacts, suggesting that the ventrolateral hypothalamus may influence steroid-dependent behaviors via the modulation of estrogen receptor-containing cells. Furthermore, ventrolateral hypothalamic projections may include direct connections with estrogen receptor-containing cells, suggesting the presence of a network of interconnected estradiol-sensitive neurons involved in the regulation of estradiol-dependent functions.

## Introduction

Estradiol and progesterone secreted by the ovaries act synergistically to regulate female sexual behavior. In the brain, intracellular receptors for ovarian steroid hormones mediate some of their behavioral effects [1]. Receptors for estradiol and progesterone have been found in many species including guinea pigs, rats, and hamsters

KARGER

Fax + 41 61 306 12 34
E-Mail karger@karger.ch
www.karger.com


0028–3835/99/0691–0063$17.50/0

Accessible online at:
http://BioMedNet.com/karger

Jeffrey D. Blaustein
Center for Neuroendocrine Studies and Neuroscience and Behavior Program
Tobin Hall – Box 37720, University of Massachusetts
Amherst, MA 01003-7720 (USA)
Tel. +1 413 545 1524, Fax +1 413 545 0769, E-Mail blaustein@cns.umass.edu

[2–9]. Ovarian steroid hormone receptors have been localized in many regions, which include the preoptic area (POA), bed nucleus of the stria terminalis (BST), amygdala, the mediobasal hypothalamus, and midbrain central gray (MCG). These and other regions sensitive to steroid hormones have been implicated in sexual behavior [10].

One region within the mediobasal hypothalamus, the ventrolateral hypothalamus (VLH) in female guinea pigs, like the analogous ventrolateral ventromedial hypothalamus (VMHVL) in rats, contains a high density of estrogen receptor- and progestin receptor-immunoreactive neurons. This region has been shown to be both necessary and sufficient for female sexual behavior. While lesions of this area abolish sexual receptivity [11–14], electrical stimulation can facilitate sexual behavior [15]. Furthermore, estradiol implants in the VLH of guinea pigs [16] and the VMHVL in rats [17–19] are sufficient for progesterone-facilitated sexual behavior.

The VLH in guinea pigs includes an estrogen receptor-containing region. This area consists of the ventrolateral nucleus (VLN) and rostrally, a band of cells lateral to the ventromedial hypothalamus, which extends from the VLN to the perifornical region. The VMHVL [20–23] as well as the region of the VLH in guinea pigs [24, 25] has been reported to project to other brain regions where estrogen receptor-containing cells have been localized [2–6, 9, 26]. Many of those regions also project back to the VLH or VMHVL, forming reciprocally connected pathways [27–29].

Hypothalamic projections from the guinea pig VLH terminating in other estrogen receptor-containing regions [24] include projections from estrogen receptor-containing cells [26]. These projections suggest the possibility that steroid hormone receptor-containing cells may be directly linked. The functional significance of these projections within the steroid-sensitive interconnected circuit is not clear. However, the correlation of anatomical and behavioral data suggests that this complex pattern of steroid hormone-sensitive neuronal pathways may mediate steroid hormone-dependent behaviors such as female sexual behavior [10, 30, 31]. This network could provide both a direct and indirect pathway for the transmission of information relevant to steroid hormone effects on behavior. It may function, at least in part, by providing a means for a wide variety of neuronal inputs at various neuroanatomical levels necessary to modulate hormonal and behavioral responses.

In order to investigate the projections of the estrogen receptor-containing region of the VLH in guinea pigs, the anterograde tracer, *Phaseolus vulgaris* leucoagglutinin (Pha-L), was deposited iontophoretically into the area within the VLH containing the high density of estrogen receptor-containing neurons. *P. vulgaris* leucoagglutinin immunoreactivity (Pha-Lir) and estrogen receptor immunoreactivity (ERIR) were then colocalized in a dual-label immunocytochemical procedure. The presence of ERIR within the cytoplasm of many neurons enabled us to visualize Pha-L-labeled terminal boutons closely associated with ERIR cells.

## Materials and Methods

*Animals*

Eleven female Hartley guinea pigs, 350–450 g, obtained from Charles River (Wilmington, Mass., USA), were group housed in a 14/10 h light/dark cycle. Food and water were freely available. All animals were ovariectomized through bilateral dorsal incisions under either sodium pentobarbital (15.1 mg/kg) and chloral hydrate (73.3 mg/kg) anesthesia or a combination of ketamine and xylazine. Prior to ovariectomy, a combination of droperidol (2%), fentanyl (0.04%), methylparaben (0.18%), and propylparaben (0.02%) in 0.04 ml was injected intramuscularly as a muscle relaxant. Anesthesia was supplemented with methoxyflurane (Metofane, Pittman Moore, Inc., Washington Crossing, N.J., USA) when necessary. All animal procedures were in compliance with guidelines of the National Institutes of Health and were approved by the University of Massachusetts Institutional Animal Care and Use Committee.

One week after ovariectomy, animals were again anesthetized with sodium pentobarbital (15.1 mg/kg) and chloral hydrate (73.3 mg/kg). Pha-L (Vector Laboratories, Burlingame, Calif., USA; 25 μg/ml dissolved in 0.01 *M* sodium phosphate buffer) was deposited iontophoretically into the VLH under stereotaxic guidance. Pha-L was ejected from glass micropipets (tip diameter 15–20 μm) with 5 μA of positive current provided by a precision current source (Transkinetics, Canton, Mass., USA). Alternating current was applied 7 s on and 7 s off for 10 min. Stereotaxic coordinates were: 0.6 mm caudal to bregma, 1.9 mm lateral to the midline, and 3.1 mm dorsal to the interaural line.

*Perfusion*

Ten days to 2 weeks were allowed for the transport of Pha-L. Animals were deeply anesthetized with an overdose of sodium pentobarbital (89 mg/kg) and chloral hydrate (425 mg/kg). They were then injected with 5,000 IU of heparin in 1 ml saline directly into the heart, and perfused intracardially. After clamping the descending aorta, animals were perfused with 150 ml of 0.15 *M* saline followed by 350 ml of 4% paraformaldehyde with or without picric acid (15% saturated) or 0.1% glutaraldehyde. The flow rate was maintained at 25 ml/min at 100 mm Hg. Brains were removed and allowed to sink overnight in 0.1 *M* Sorensen's buffer with 20% sucrose in preparation for microtome sectioning. Sections were stored in 0.05 *M* Tris-buffered saline (TBS) pH 8.6.

*Immunocytochemistry*

*Pha-L Immunocytochemistry.* In an immunocytochemical technique adapted from De Vries et al. [32], free-floating, 40- or 50-μm

sections were rinsed with TBS pH 8.6. TBS pH 8.6 was used throughout the pretreatment for all solutions and washes. To remove residual aldehydes, sections were treated with 0.1% sodium borohydride (15 min) followed by 10% normal rabbit serum (Arnel), 3% Triton X-100 (TX) and 1% hydrogen peroxide (10 min). This step blocked nonspecific immunostaining, increased tissue permeability and quenched endogenous peroxidase activity, respectively. Sections were then incubated for 2 days in Pha-L antibody (1:2,000; Vector Laboratories) in TBS pH 8.6 at 4°C, with 2% normal rabbit serum and 0.3% TX. Following incubation in the primary antibody, sections were rinsed (2 × 5 min) in TBS with 0.3% TX and 0.1% gelatin (pH 8.6) and once in TBS pH 7.6. Sections were then incubated in biotinylated rabbit anti-goat IgGs (1:200; Vector Laboratories) for 45–90 min. Sections were rinsed (2 × 5 min) in TBS pH 7.6 with 0.3% TX and 1% gelatin and (1 × 5 min) in TBS pH 7.6 before incubation in avidin DH-biotinylated horseradish peroxidase H complex (ABC standard elite kit, Vector Laboratories). Pha-L was visualized after incubation in diaminobenzidine (DAB) with nickel ammonium sulfate, which resulted in a deep blue reaction product.

*Controls:* In order to insure that there was no cross-reactivity with endogenous antigens, the Pha-L antiserum, the primary antibody and the biotinylated rabbit anti-goat serum were omitted separately from the immunocytochemical procedure. Pha-L immunostaining was completely eliminated in these control procedures [24].

*Estrogen Receptor Immunocytochemistry.* Sections immunostained for Pha-L were pretreated in 10% dimethylsulfoxide to increase permeability followed by a second blocking step in TBS with 1% normal goat serum and bovine serum albumin. Following pretreatment, sections were incubated in H 222 antibody diluted (5 μg/ml) in 0.05 *M* TBS with 0.02% sodium azide, 0.05% TX, and 0.1% gelatin pH 7.6 at 4°C. Three days later, sections were incubated in goat anti-rat IgGs for 30 min followed by 30 min in rat peroxidase-antiperoxidase complex in a multiple-bridge procedure as described previously [33]. The buffer used to dilute secondary and tertiary antisera and for washes between incubations was the same as that used for the primary antibody (pH 7.6 at room temperature). Buffer without gelatin was used for rinses before incubation in 0.05 *M* TBS with 0.05% DAB and 0.05% hydrogen peroxide.

In a streptavidin procedure used for some of the brains, multiple bridging of secondary and tertiary antibodies was not required resulting in improved cytoplasmic immunostaining for estrogen receptors and reduced nonspecific background. For this protocol, sections were removed from primary antibody rinsed and incubated in biotinylated rabbit anti-rat IgGs (1:200; Vector Laboratories). One hour later, sections were rinsed as described above and incubated in avidin DH-biotinylated horseradish peroxidase H complex (1:150; Vector Laboratories) for 1 h. After a final set of rinses, tissue was reacted in DAB and hydrogen peroxide. Sections were mounted on slides and coverslipped with Permount for light microscopic examination.

*Controls:* Controls for the specificity of the H 222 antibody have been previously described in detail [33, 34] and included preadsorption of the antibody with a cellular extract of yeast cells expressing high levels of estrogen receptors. The omission of either the primary antibody (H 222) or the secondary antibody (biotinylated goat anti-rat with or without biotin) eliminated all specific estrogen receptor immunostaining. The use of pH 8.6 for the Pha-L technique improved sensitivity of the procedure; combined with the use of a high pH in the nickel DAB incubation, this results in bluish purple Pha-L immunostaining in fibers and punctate structures. This was easily distinguishable from the ERIR, which was brown. As observed earlier [33], ERIR was very dense in cell nuclei with some light brown immunoreactivity present in cytoplasmic processes proximal to the cell soma (see fig. 3A–C).

*Camera lucida Drawings*

A drawing tube was used to make reconstructions of labeling from three levels through the brain, preoptic area, hypothalamus and midbrain. Additional drawings were also made at three levels through the midbrain central gray. All drawings were made from 1 animal with a Pha-L deposit accurately placed in the VLH. This animal was chosen because the high density of Pha-L-labeled fibers would ensure that areas with low levels of immunostaining would be detected. All fibers and estrogen receptor-containing cells in each section were included in each drawing. However, the numerous Pha-Lir boutons observed throughout the brain were omitted to avoid obscuring the estrogen receptor-containing cells. The drawings illustrate the distributions of fibers and cells and anatomical detail were depicted in high-power photomicrographs.

Anatomical landmarks were drawn from immunostained sections with the aid of dark-field and phase-contrast microscopy. Landmarks were also verified in adjacent sections labeled with Pha-L alone and in matched sections from other animals labeled with stain for Nissl substance. The nomenclature was taken from the rat atlas of Paxinos and Watson [35] with the exceptions of the following terms: VLN was taken from the guinea pig forebrain atlas of Bleier [36], and VLH was used to denote the estrogen receptor-containing region outside the VMN, which is not well defined cytoarchitecturally. Although the anatomy of the rat and guinea pig may be similar but not necessarily analogous, the nomenclature from the rat atlas was used because the available guinea pig atlases were too limited in scope.

## Results

Eleven guinea pigs had Pha-L deposits overlapping the estrogen receptor-rich area within the VLH, of which 4 guinea pigs had Pha-L deposits centered directly over the estrogen receptor-rich area (fig. 1). These animals were chosen for the analysis of projections to other estrogen receptor-containing regions. The resulting Pha-L immunostaining among the 4 animals analyzed was very similar with respect to the location of labeled fibers, although the density of Pha-Lir fibers varied.

Efferent projections from the VLH, including those from ERIR cells, were mapped in transverse sections from 3 animals and sagittal sections from 1 animal (fig. 1). Pha-Lir was found primarily ipsilateral to the injection site. Some labeling was also observed in identical contralateral regions, especially in the MCG. Projections from the VLH were widespread and overlapped to a large extent with the distribution of ERIR neurons. VLH projections terminate extensively within the hypothalamus itself, as described previously in rats [37–39], and throughout the basal forebrain and dorsal midbrain [24].

*Abbreviations used in table 1 and figures 1–8*

| | |
|---|---|
| 3V | third ventricle |
| ac | anterior commissure |
| Aco | anterior cortical amygdaloid nucleus |
| AHA | anterior hypothalamic area, anterior |
| AHP | anterior hypothalamic area, posterior |
| AMPO | anterior medial preoptic nucleus |
| APT | anterior pretectal nucleus |
| Aq | aqueduct |
| ARC | arcuate hypothalamic nucleus |
| AV | anteroventral thalamic nucleus |
| bic | brachium inferior colliculus |
| BMA | basomedial amygdaloid nucleus |
| BST | bed nucleus stria terminalis |
| BSTI | bed nucleus stria terminalis, intermediate div. |
| BSTIA | bed nucleus stria terminalis, intermediate amygdaloid div. |
| BSTLV | bed nucleus stria terminalis, lateral ventral div. |
| BSTMA | bed nucleus stria terminalis, med. div., ant. |
| BSTMPI | bed nucleus stria terminalis, med. div., posteroint. |
| BSTMPL | bed nucleus stria terminalis, med. div., posterolat. |
| BSTMPM | bed nucleus stria terminalis, med. div., posteromed. |
| BSTV | bed nucleus stria terminalis, ventral div. |
| CeL | central amygdaloid nucleus, lat. div. |
| CG | central gray |
| cp | cerebral peduncle |
| ctg | central tegmental tract |
| DA | dorsal hypothalamic area |
| DK | nucleus Darkschewitsch |
| DMD | dorsomedial hypothalamic nucleus, diffuse part |
| DpG | superior colliculus, deep gray layer |
| DpMe | deep mesencephalic nucleus |
| DpWh | superior colliculus, deep white layer |
| DR | dorsal raphe nucleus |
| dtg | dorsal tegmental bundle |
| ER | estrogen receptor |
| ERIR | estrogen receptor immunoreactive |
| EW | Edinger-Westphal nucleus |
| f | fornix |
| ic | internal capsule |
| InG | intermediate gray layer superior colliculus |
| InWh | superior colliculus, intermediate white layer |
| LH | lateral hypothalamic area |
| LPO | lateral preoptic area |
| LHb | lateral habenular nucleus |
| MA3 | medial accessory oculomotor nucleus |
| MCG | midbrain central gray |
| MCPO | magnocellular preoptic nucleus |
| MeA | medial amygdala nucleus |
| MePV | medial amygdala nucleus, posteroventral |
| mfb | medial forebrain bundle |
| MG | medial geniculate nucleus |
| Min | minimus nucleus |
| ml | medial lemniscus |
| mlf | medial longitudinal fasciculus |
| MnPO | median preoptic nucleus |
| MPA | medial preoptic area |
| mt | mammillothalamic tract |
| opt | optic tract |
| ox | optic chiasm |
| PaMP | paraventricular hypothalamic nucleus, med. parvocell. |
| Pe | periventricular nucleus |
| PH | posterior hypothalamic area |
| Pha-L | *Phaseolus vulgaris* leucoagglutinin |
| Pha-Lir | *Phaseolus vulgaris* leucoagglutinin immunoreactive |
| PMV | premamillary nucleus, ventral part |
| PP | peripeduncular nucleus |
| PPT | posterior pretectal nucleus |
| PV | paraventricular thalamic nucleus |
| Rli | rostral linear nucleus raphe |

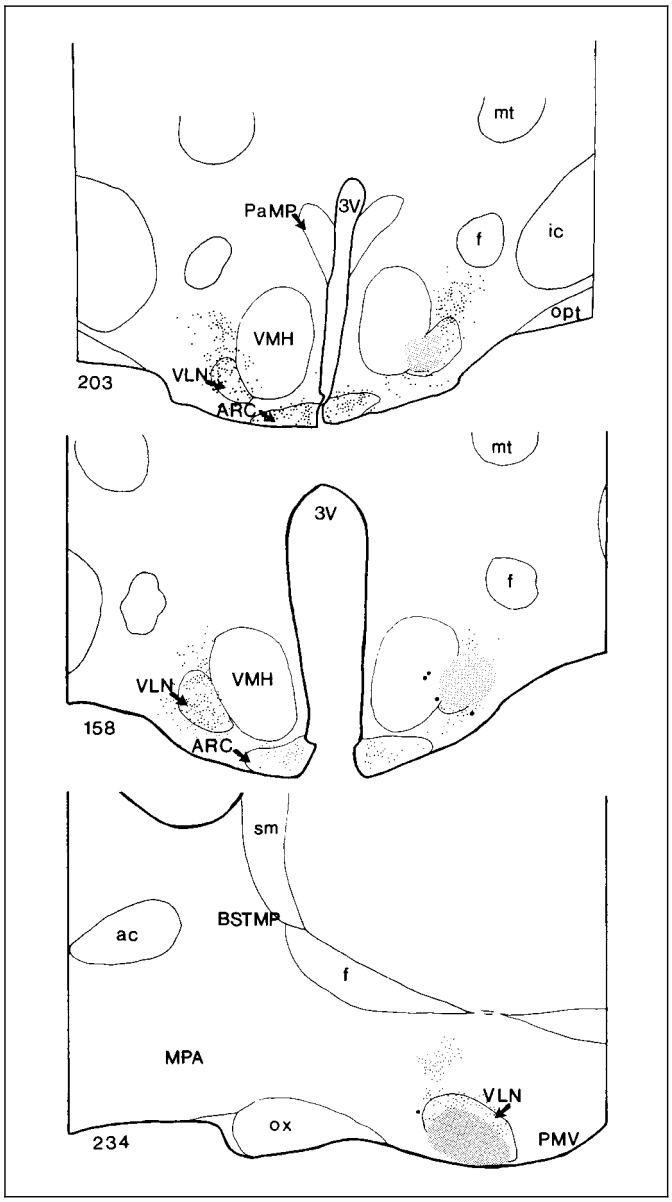


**Fig. 1.** Camera lucida drawings illustrating the location of Pha-L deposits (shading) with respect to the distribution of estrogen receptor-containing cells (small dots, each represents one cell) in guinea pig hypothalamus. Large dots represent cells outside of the Pha-L deposit which were labeled by Pha-L.

| | |
|---|---|
| RMC | red nucleus, magnocellular |
| Rpn | raphe pontis nucleus |
| SC | superior colliculus |
| sm | stria medullaris |
| SNC | substantia nigra, compact |
| SNR | substantia nigra, reticular |
| VLH | ventrolateral hypothalamus |
| VLN | ventrolateral hypothalamic nucleus |
| VMN | ventromedial hypothalamic nucleus |
| VTA | ventral tegmental area |
| Zi | zona incerta |

**Table 1.** Relative densities of Pha-L and ERIR in specified sites in guinea pig brain; relative densities of Pha-Lir in VLH projection sites are indicated as low (+), moderate (++), and high (+++)

| VLH projection site | Pha-L density | ERIR |
|---|---|---|
| MPA | +++ | ++ |
| AMPO | ++ | +++ |
| MnPO | + | ++ |
| LPO | + | + |
| BSTMA | +++ | ++ |
| BSTV | ++ | ++ |
| BSTMPM | + | +++ |
| BSTMPI | +++ | ++ |
| BSTMPL | +++ | ++ |
| AHA | +++ | ++ |
| AV | + | ++ |
| PaMP | ++ | ++ |
| MeA | + | +++ |
| BMA | + | +++ |
| Aco | + | +++ |
| CeL | ++ | + |
| DA | ++ | + |
| ZI | ++ | + |
| VMN | +++ | + |
| VLH | +++ | +++ |
| ARC | + | +++ |
| PV | + | |
| LHb | + | |
| DMD | ++ | + |
| PH | ++ | + |
| VTA | + | ++ |
| PP | ++ | ++ |
| SC | ++ | ++ |
| MCG | | |
| Dorsal | +++ | +++ |
| Lateral | ++ | +++ |
| Ventrolateral | ++ | ++ |
| Ventral | + | + |

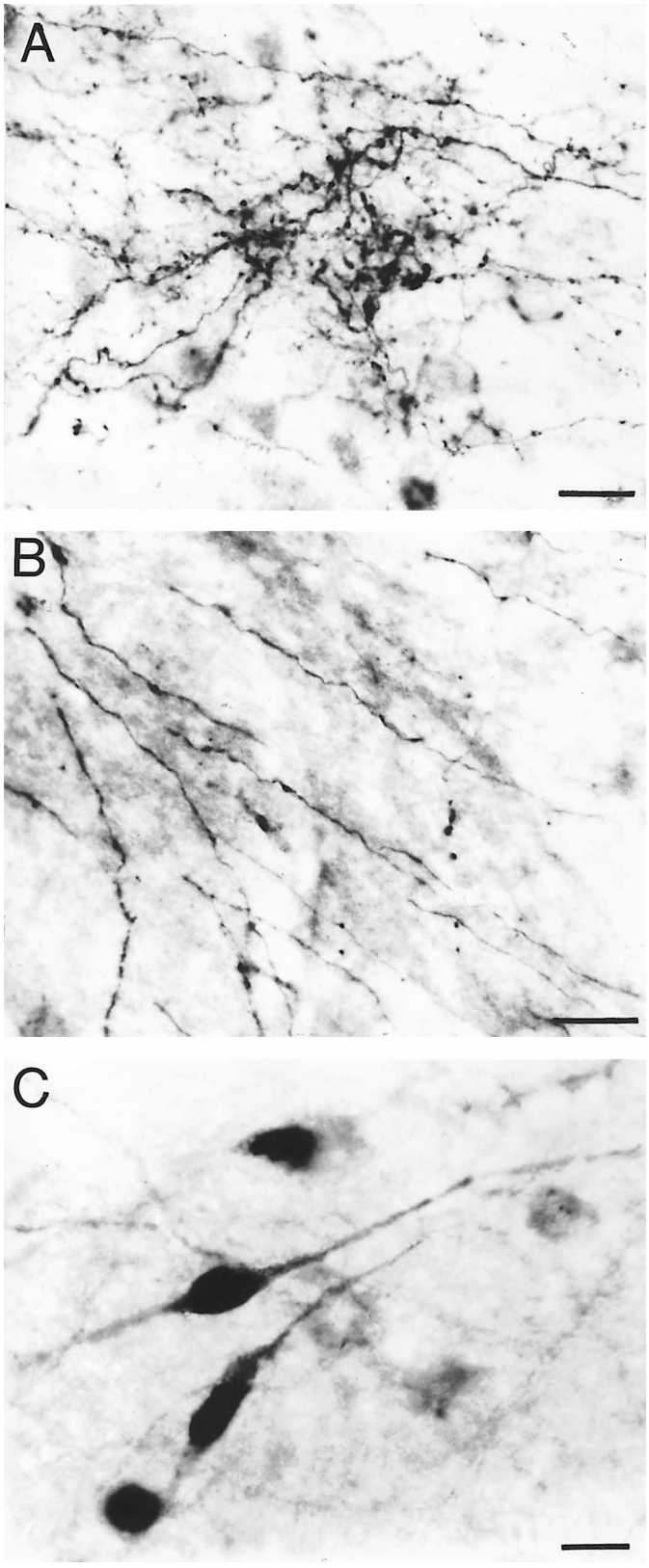


**Fig. 2.** Photomicrographs showing the difference between (**A**) terminal fields, (**B**) fibers of passage and (**C**) estrogen receptor-containing cells in the MCG. The terminal field was from the medial tuberal region of the hypothalamus where fibers branch substantially and have numerous putative terminal boutons and varicosities. The fibers of passage, shown here, follow the optic tract and enter amygdala. Scale bar = 50 μm. Estrogen receptor-containing cells in the MCG have very dark nuclei and lightly stained cytoplasm. Scale bar = 10 μm.

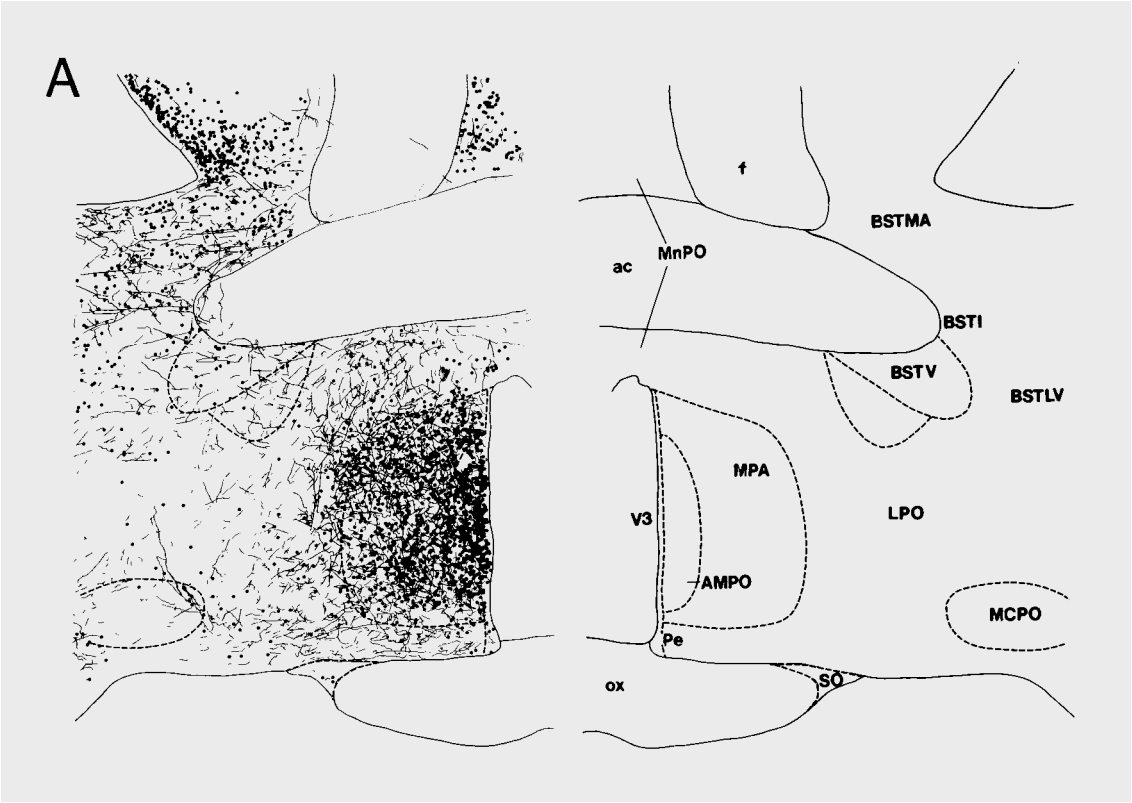


**Fig. 3.** Camera lucida drawings representing the distribution of estrogen receptor-containing cells (dots) and Pha-L-labeled fibers (lines) at three levels of the brain of animal 206: (**A**) POA, (**B**) VMN and (**C**) rostral midbrain. Each dot represents one estrogen receptor-containing cell.

*VLH Projections to Estrogen Receptor-Containing Regions*

Terminal fields, where Pha-L-labeled axons branched extensively and had numerous varicosities and/or putative terminal boutons (fig. 2A), were easily distinguished from areas with fibers of passage, which had few or no terminals (fig. 2B). Estrogen receptor-immunoreactive cells were also easily identified and differentiated from fibers of passage and terminal fields by their large nuclei and lightly immunostained cytoplasmic processes (fig. 2C).

Estrogen receptor-containing cells were widely distributed throughout the mediobasal hypothalamus and midbrain. The distribution of these cells has been described [3, 34, 40]. Most regions with ERIR were also regions in which VLH fibers and boutons could be found in varying densities (table 1). The highest degree of overlap between estrogen receptor-containing regions and VLH projections included the MPA, the BST, the VLH and the MCG. Estrogen receptor-containing regions with low densities of fibers and terminals included the arcuate and the amygdala. Some Pha-L-labeled varicosities were found closely associated with ERIR cells in all these regions. The density of the VLH innervation of ERIR regions was not uniform, and some regions in which Pha-Lir and ERIR overlap are described below in rostral to caudal order.

*VLH projections to the preoptic area:* The intensity of Pha-Lir and ERIR varied greatly within the preoptic region. For example, the density of fibers and boutons in the MPA was high (fig. 3A, 4). However, in the adjacent anteromedial nucleus the density of fibers and boutons decreased, and the density of ERIR cells increased. In the median preoptic nucleus, there was a moderate density of ERIR cells but almost no Pha-L-labeled fibers, while the densities of both Pha-Lir and ERIR in the lateral preoptic area were low (fig. 3A).

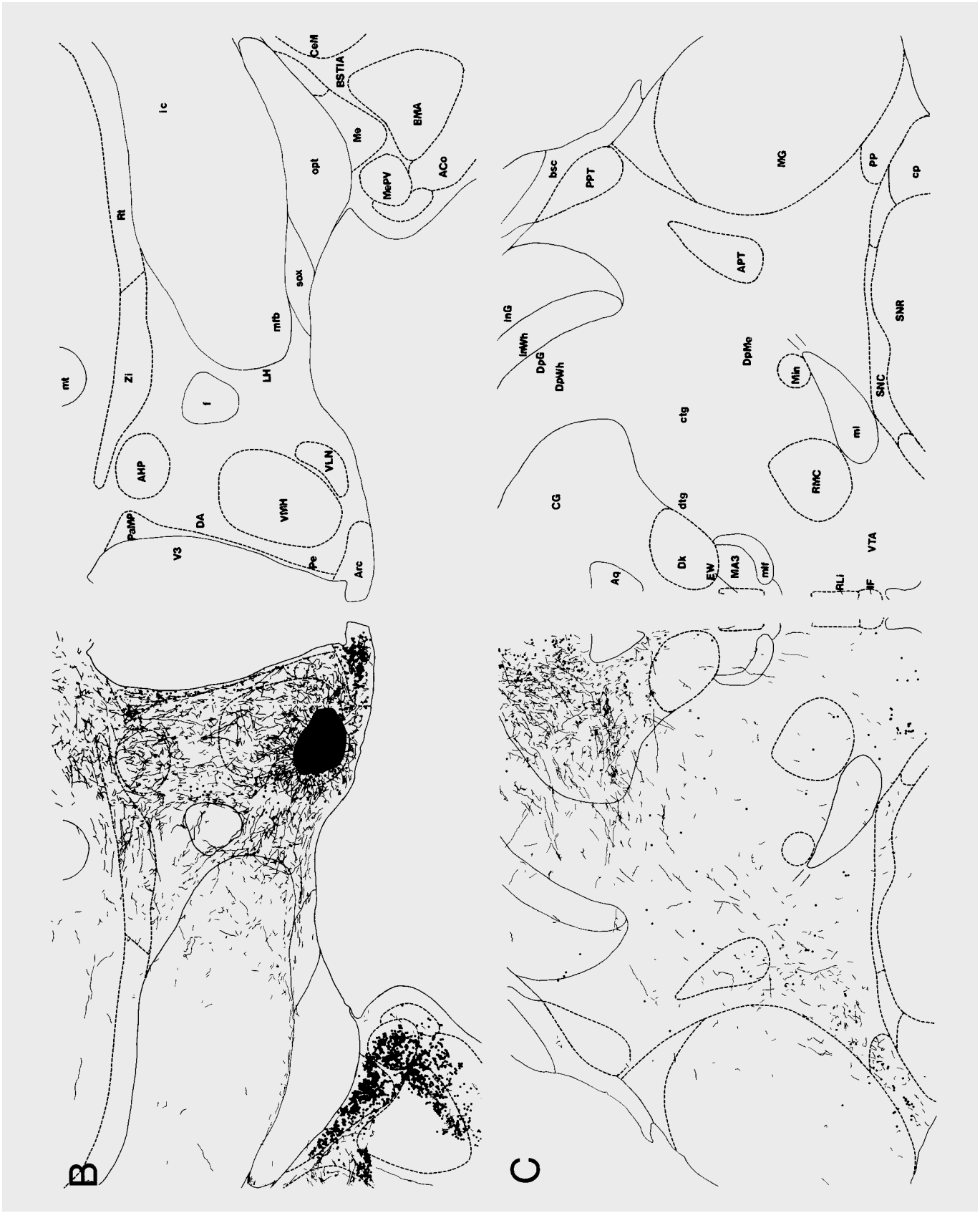
B
mt
ZI
Rt
ic
f
LH
mfb
sox
opt
Me
MePV
BMA
ACo
CeM
BSTIA
AHP
DA
PaMP
V3
VMH
VLN
Pe
Arc
C
bsc
PPT
MG
PP
cp
APT
inG
inWh
DpG
DpWh
DpMe
Mln
SNC
SNR
ml
ctg
CG
dtg
Dk
EW
MA3
mlf
RtMC
Aq
RLi
IF
VTA

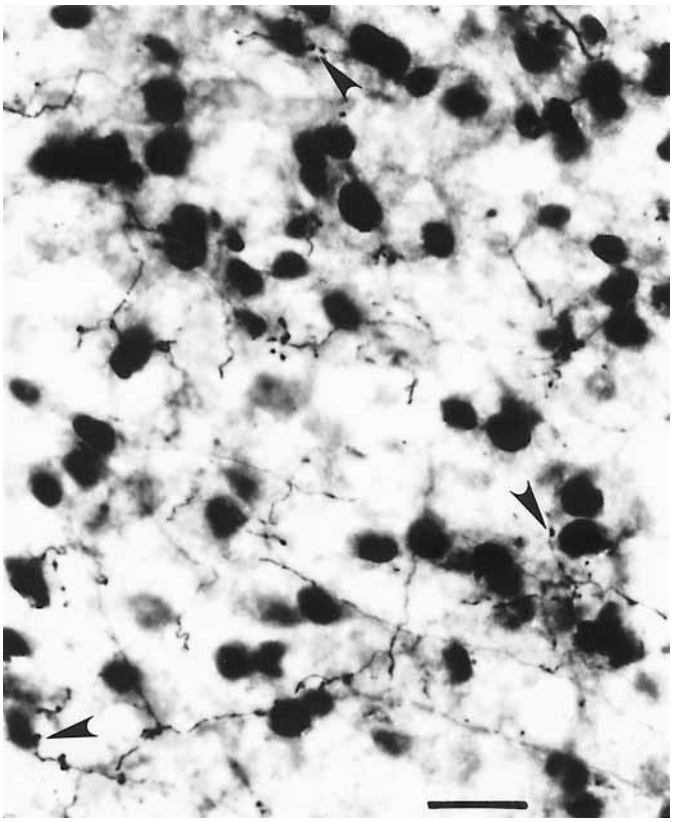

**Fig. 4.** High-power photomicrograph of Pha-Lir and ERIR in the medial preoptic area. Estrogen receptor-containing cells, Pha-L-labeled fibers and putative synaptic contact (arrowheads) are densest in this region. Scale bar = 50 μm.

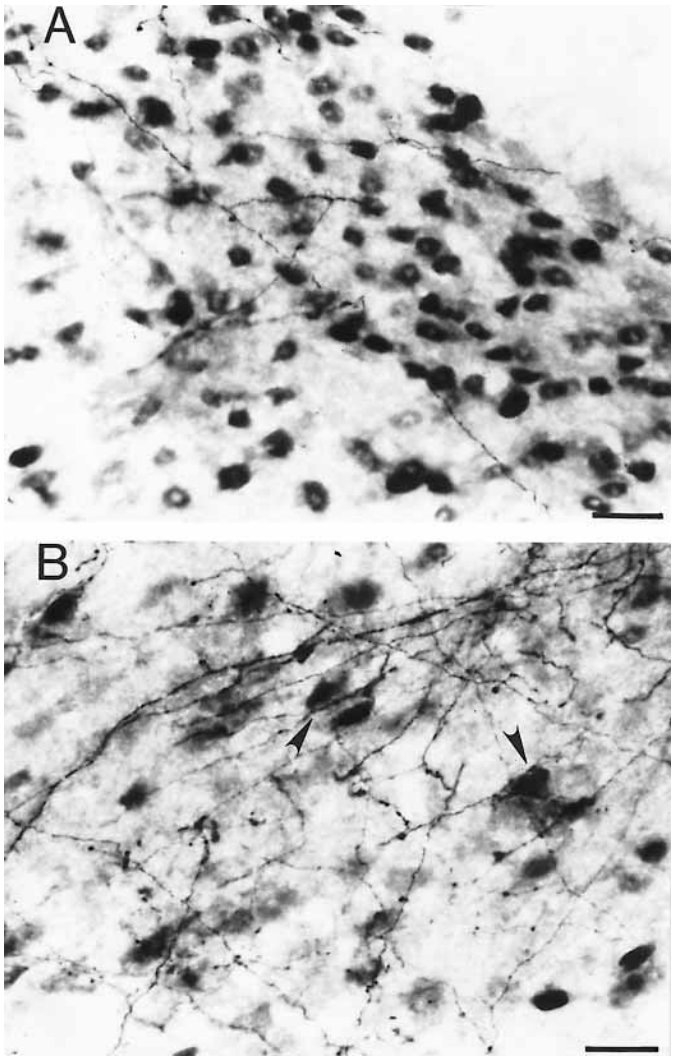


**Fig. 5.** Photomicrographs of two regions within the BST: (**A**) the medial posteromedial division and (**B**) the ventral division. Estrogen receptor-containing cells in the medial posteromedial division are densely packed with a few Pha-L fibers of passage. In the ventral division, estrogen receptor-containing cells of large diameter are more widely scattered. Many Pha-L fibers are found in this area. These fibers appear to be descending from the stria terminalis and many varicosities appear to be closely associated with estrogen receptor-containing cells (arrowheads). Scale bar = 50 μm.

The anterior medial division (fig. 5) and the posteromedial divisions of the BST were heavily labeled with Pha-Lir projections from the VLH. The ventral and ventrolateral divisions were moderately labeled (fig. 5). Pha-Lir varicosities were frequently observed in close apposition to ERIR cells with some variation (fig. 5, 6B). Pha-Lir fibers were moderately low where small diameter ERIR cells were most dense in the BST in the medial posteromedial division (fig. 5A). Pha-Lir was more dense in the medial posterior intermediate and medial posterolateral divisions. These fibers coursed through the stria terminalis into the BST and continued into the MPA. Some fibers also seemed to pass behind the anterior commissure, possibly forming projections to the contralateral side of the BST and MPA. Varicosities and boutons *en passant* were observed along the length of some fibers. In these lateral posterior divisions of the BST, ERIR cells tended to be larger in diameter and more scattered than in the medial posteromedial division and were found embedded in fibers crisscrossing the ventral division of the BST (fig. 5B). Many ERIR cells appear to have Pha-L-labeled boutons in close association (fig. 6B).

*VLH projections to the amygdala:* The density of ERIR cells in the amygdala was high, especially in the medial nuclei. However, the density of Pha-L-labeled fibers was

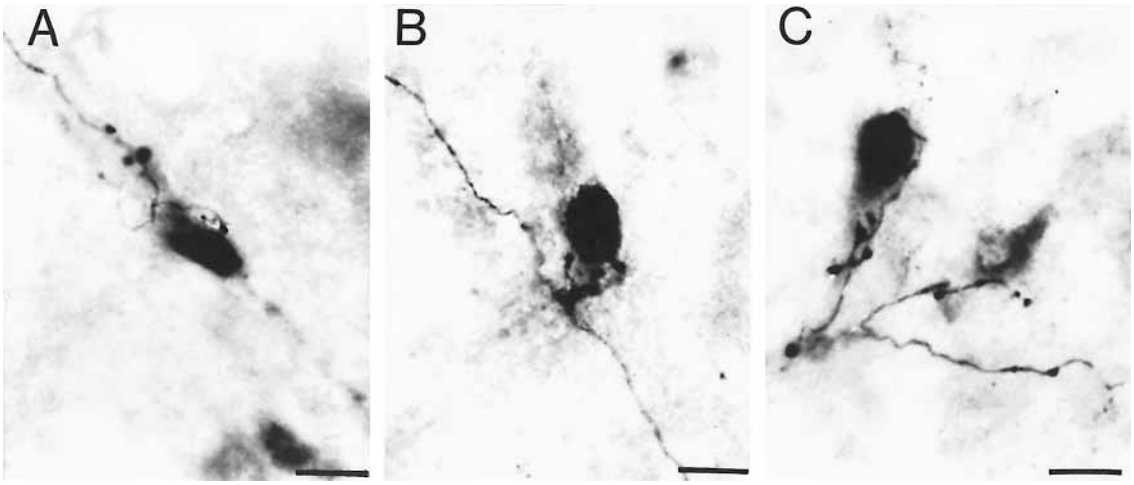


**Fig. 6.** High-power photomicrographs of Pha-L-labeled terminals closely associated with estrogen receptor-immunoreactive cells in the (**A**) BST, (**B**) the amygdala, and (**C**) the ventrolateral hypothalamus contralateral to the injection site. Scale bar = 10 μm.

low with sparse terminals in the medial amygdala (fig. 3B), basomedial, anterior cortical nuclei and the region surrounding the central amygdala, including the lateral capsular division. There appeared to be more terminals in the amygdaloid division of the BST and the dorsal medial amygdala closely associated with ERIR cells than in other nuclei. The fibers that entered the amygdala, although sparse, seemed to form terminals adjacent to ERIR cells (fig. 6C).

*VLH projections to the hypothalamus*: Projections from the VLH also formed varicosities and terminals throughout the anterior hypothalamus. Some of these boutons seemed to form close appositions with large ERIR cells scattered throughout this region. However, the varicosities and boutons were fairly dense and frequently found independent of ERIR cells. Moderate levels of Pha-L-labeled fibers and boutons were observed in the paraventricular nucleus (fig. 3B). In this area some ERIR cells were found closely associated with terminal boutons, especially in the anterior ventral and medial parvocellular divisions.

Moderate densities of Pha-Lir fibers and terminals were also observed in other regions containing ERIR. These regions included the dorsal and posterior hypothalamic areas and the zona incerta, which contained a low density of ERIR cells (fig. 3B).

The VMN, especially the anterior VMN, contained a fairly high density of projections from the adjacent VLH, but contained few ERIR cells. The density of Pha-Lir fibers and terminals seemed higher in the region where ERIR cells were found, in the VLN and the region lateral to the VMN (fig. 3B). ERIR cells in the VLH were closely associated with boutons, both rostral and caudal to the Pha-L injection site. Interestingly, the VLH contralateral to the injection site also contained labeled boutons and fibers (fig. 6A) even though the contralateral VMN was not labeled.

*VLH projections to the arcuate nucleus:* The arcuate nucleus, like the amygdala, contained a high density of ERIR cells, but few projections from the VLH (fig. 3B). The majority of the few ERIR cells with adjacent Pha-L-labeled boutons were found in the rostral arcuate nucleus. The caudal arcuate region seemed to have very little Pha-L labeling. Regions with Pha-Lir fibers and terminals, but no apparent ERIR labeling, included the mediodorsal thalamus, paraventricular thalamus and the region of the habenular nuclei.

*VLH projections to the MCG:* ERIR cells were found in the dorsal, lateral and ventrolateral divisions of the MCG. All of these divisions received projections from the VLH. The most dense projections were found in the rostral third of the dorsal MCG (fig. 3C, 7A). Pha-Lir fibers entered dorsally and formed dense terminal fields within the dorsal half of the MCG. Close associations with ERIR cells were difficult to determine in this region due to the density of projections and the absence of ERIR in cytoplasmic processes in this region.

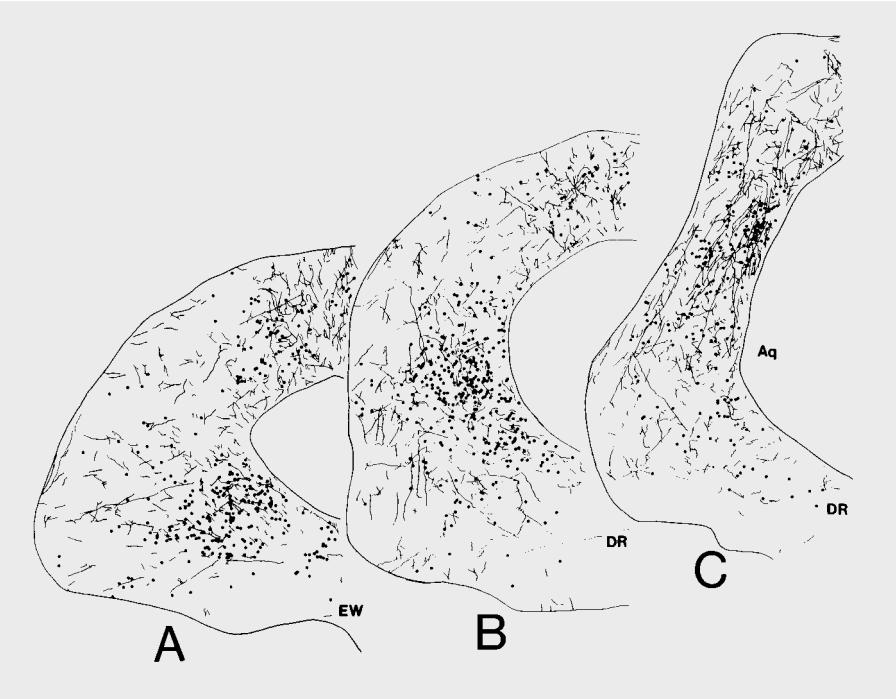


**Fig. 7.** Camera lucida drawings illustrating the overlap of Pha-L-labeled fibers and estrogen receptor-containing cells at three levels of the MCG: (**A**) rostral intercollicular level, (**B**) caudal MCG, and (**C**) the level of the recess of the inferior colliculus.

ERIR cells in the lateral MCG, in contrast to those in the dorsal division, did show cytoplasmic immunostaining as well as nuclear staining (fig. 8A, B). Pha-L-labeled boutons were found closely associated with some of these cells.

At the intercollicular level of the MCG, the dorsal projections descending into the mediodorsal MCG were less dense, although the number of ERIR cells was fairly constant. However, in the lateral MCG, the number of ERIR cells with cytoplasmic immunostaining increased with a concomitant increase in apparent Pha-L-labeled fibers and boutons. These cells are closely associated with boutons and varicosities of fibers which passed both caudally parallel to the cerebral aqueduct and fibers, and which cross the central gray extending toward the cerebral aqueduct at right angles to the parallel fiber stream (fig. 7B, 8A). Some ERIR cells were present at this level in the ventrolateral MCG as well as the lateral division.

ERIR cells within the caudal MCG were more numerous in the lateral and ventrolateral divisions. Pha-Lir fibers were dense throughout these areas and continued to be found closely associated with ERIR cells (fig. 7B).

At the level of the inferior collicular recess, VLH fibers continued to descend through the dorsal MCG, and few fibers entered laterally (fig. 7C, 8B). Some fibers formed terminals in the medial portion of the MCG adjacent to the aqueduct, while others passed directly into the ventrolateral MCG. The most cohesive group of ERIR cells was found lateral to the cerebral aqueduct. However, there were also ERIR cells in the dorsal and ventrolateral MCG. As was the case throughout the MCG, ERIR cells in the dorsal region were in an area with fairly dense boutons. The ERIR cells in the ventrolateral MCG were more widely dispersed and did not seem to be associated with Pha-Lir boutons. The majority of Pha-Lir fibers traveled ventrolaterally and exited the MCG in the region of the cuniform nucleus descending to the medulla and spinal cord.

## Discussion

Projections from the estrogen receptor-rich VLH in female guinea pigs were found in many other regions in which estrogen and progestin receptors are found. The efferent projections of the VLH were very similar to those previously described for this area in guinea pigs [24, 25] and for the potentially analogous VMHVL of rats [22, 23, 41–44]. In contrast to previous studies, we combined anterograde tract tracing and steroid hormone receptor immunocytochemistry in order to carefully delineate the overlap of terminals of neurons in the estrogen receptor-

rich area of the VLH with estrogen receptor-containing cells in other regions. Based upon earlier work, it was assumed that the estrogen receptor-rich VLH would project to other regions containing estrogen receptors. We have confirmed these findings in female guinea pigs. Moreover, we also observed that many of these projections were closely associated with estrogen receptor-containing neurons.

Pha-Lir in projections from the VLH was observed in varying densities in terminals in all regions where ERIR cells were also found. The abundance of Pha-Lir varicosities and boutons was not always correlated with the density of ERIR cells in a particular area. For example, the arcuate nucleus and the amygdala have high concentrations of ERIR neurons, yet the density of Pha-Lir fibers and boutons is low. There were also some apparent projection sites from the VLH in which ERIR was not observed. Areas without apparent ERIR included the mediodorsal and paraventricular nuclei of the thalamus and habenular region. Alternatively, ERIR neurons, but few apparent Pha-Lir fibers, were observed in the ventral tegmental area.

In virtually every projection site of the VLH in which ERIR neurons were found, Pha-Lir terminal boutons and perineuronal baskets were found closely associated with ERIR cells. Pha-L has been reported to fill axons, and terminal swellings labeled with Pha-L have been shown to be synaptic boutons [45, 46]. Thus, the close associations between Pha-L-labeled boutons and ERIR cells strongly suggest the presence of synaptic contacts. While these synaptic associations were categorized by relative densities, we did not attempt a more detailed quantification of these interactions, because of differences in the size of the Pha-L deposit. Unfortunately, variability in the size of the Pha-L deposit, the number of VLH cells which picked up the tracer, and in immunostaining can result in variability among animals. Furthermore, although our immunocytochemical procedure stains some ERIR cell processes as well as nuclei, usually there is a great deal of variability in the extent of cytoplasmic estrogen receptor immunostaining. In fact, ERIR cells in some brain regions do not exhibit any cytoplasmic staining [47]. As a result of this limitation, which prevents the visualization of entire dendritic arbors, any estimate of the number of ERIR cells with closely associated Pha-Lir boutons would be an underestimate.

Although the VLH is rich in estrogen receptor-containing cells, it is also a heterogeneous region with cells that contain estrogen receptors as well as cells that do not. Consequently, since there is no method currently avail-

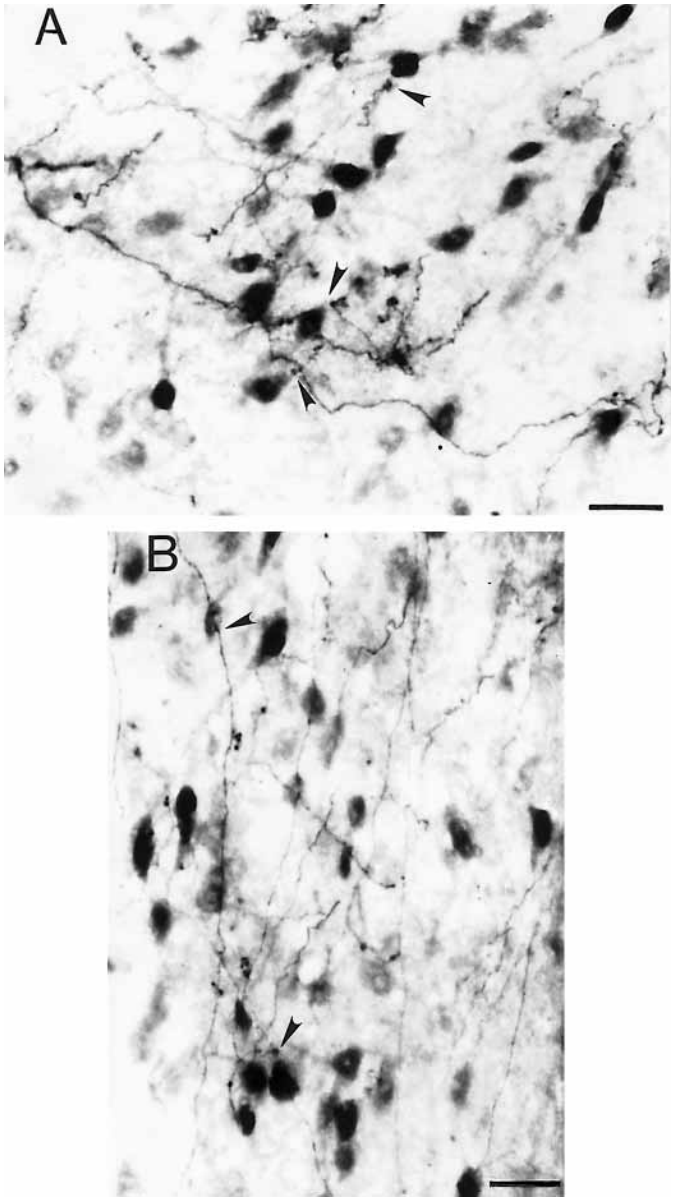


**Fig. 8.** High-power photomicrographs at two levels of the MCG. **A** At the intercollicular level Pha-L fibers form right angles and cross the central gray. These fibers have varicosities, some of which seem to be adjacent to estrogen receptor-immunoreactive cells (arrowheads). **B** At the level of the recess of the inferior colliculus, most Pha-L fibers enter the dorsal MCG and descend to the ventrolateral region where they exit in the area of the cuniform nucleus. Some of these fibers seem to form terminals which are closely associated with estrogen receptor-immunoreactive cells (arrowheads). Scale bar = 50 μm.

able to label exclusively estrogen receptor-containing cells with tracer, projections from the VLH included efferent fibers from both populations. Because the VLH was so heavily stained by the Pha-L, the quantification of ERIR cells containing Pha-Lir was not possible. However, the terminal fields observed were regions in which estrogen receptor-containing cells have been reported to project [26, 43, 48–50]. Thus, the location of projections from the VLH determined in this study using anterograde labeling is consistent with previous reports of projections of estrogen receptor-containing cells in the VLH.

Earlier retrograde studies reported that estrogen receptor-containing cells in the guinea pig VLH project to the MPA, BST, amygdala and MCG. Although differences between this experiment and previous experiments include the sex of the animals used, the particular steroid hormone receptor investigated (estrogen receptor or progestin receptor), species (rat or guinea pig), and precise hypothalamic locus studied, the studies are all in agreement with the idea that the estrogen receptor-containing neurons within the general area of the VLH project to each of these areas [26, 43, 48, 50–53]. Thus, many of the estrogen receptor-containing neurons in the VLH project to those regions which also receive the heaviest projections from the VLH and also contain the largest number of boutons closely associated with ERIR cells.

Two of the major projection sites of the VLH, the MPA and the MCG, are regions that have been demonstrated as being important for sexual behavior [11, 54–56]. In particular, the MCG, the major descending projection site from the VLH, and the connections between the VLH and MCG are critical for sexual behavior. Projections from the VLH to the MCG are found throughout its rostrocaudal dimension. These projections are closely associated with estrogen receptor-containing neurons in the MCG, and their distribution seems to correspond roughly with functionally defined longitudinal columns [57–59]. The majority of close associations of VLH efferents and ERIR cells in the MCG is found in the mediodorsal column located just above the cerebral aqueduct and in the lateral and ventrolateral columns where estrogen receptor-containing neurons with immunostained cytoplasmic processes are found. In addition, MCG projections from the lateral column project to the medulla [60], a region reported to activate back muscles involved in lordosis [61] and a subpopulation of these projections originate from estrogen receptor-containing neurons [62].

The MPA, a major ascending projection site of the VLH, has an inhibitory role in sexual behavior [63–65]. While the MPA receives somatosensory input during mating [66], it has a net descending inhibitory effect on lordosis [67]. Projections from the VLH to the MPA may modulate this inhibition [52] and influence both motivational and solicitous behavior associated with reproduction. The MPA, in turn, sends projections to the ventral MCG which may inhibit sexual behavior by modulating facilitory input from the VLH [67–69]. These projections could function to modulate VLH facilitory input to this region.

Although pathways from the estrogen receptor region of the VLH have been described [30, 31], this study demonstrates the probability of direct connections between steroid hormone receptor-containing cells. In speculating on the function of this steroid-sensitive neural network, Cottingham and Pfaff [30] suggested that interconnectedness might allow for amplification of steroid hormone effects, stability of hormone-neuron system performance, and selective channeling of inputs to the network. These are not in any way mutually exclusive, and each remains a possibility. However, it is also possible that the redundancy of control by sex steroid hormones allows a means for neural input from different sensory modalities and environmental regulators to potentiate and/or inhibit the network at a wide variety of levels. For example, inputs as diverse as those conveying information about genital stimulation, olfactory stimulation, photoperiod, or nutrient availability, could each have access to the estradiol-sensitive network at independent levels. Regardless of the function of this interconnectedness of estradiol-sensitive neurons, the propensity of VLH projections to terminate within estrogen receptor-containing regions suggests that the VLH may influence steroid-dependent behaviors via connections to estrogen receptor-containing cells.

## Acknowledgments

This work was supported by NS19327 and RSDA MH01312 to J.D.B. We would like to thank Geert Devries, George Wade, Sandra Petersen and Elizabeth Connor for helpful comments on the manuscript and Robin Lempicki for technical assistance. This paper is based upon a dissertation submitted by J.C. Turcotte to the graduate school of the University of Massachusetts in partial fulfillment of requirements for a doctoral degree.

## References


1 Blaustein JD, Olster DH: Gonadal steroid hormone receptors and social behaviors; in Balthazart J (ed): Advances in Comparative and Environmental Physiology. Berlin, Springer, 1989, vol 3, pp 31–104.
2 DonCarlos LL, Greene GL, Morrell JI: Estrogen plus progesterone increases progestin receptor immunoreactivity in the brain of ovariectomized guinea pigs. Neuroendocrinology 1989;50:613–623.
3 DonCarlos LL, Monroy E, Morrell JI: Distribution of estrogen receptor-immunoreactive cells in the forebrain of the female guinea pig. J Comp Neurol 1991;305:591–612.
4 Stumpf WE, Sar M: Anatomical distribution of estrogen, androgen, progestin, corticosteroid and thyroid hormone target sites in the brain of mammals: Phylogeny and ontogeny. Am Zool 1978;18:435–445.
5 Pfaff DW, Keiner M: Atlas of estradiol-concentrating cells in the central nervous system of the female rat. J Comp Neurol 1973;151:121–158.
6 Sar M: Distribution of progestin-concentrating cells in rat brain: Colocalization of [(3)H]ORG.2058, a synthetic progestin, and antibodies to tyrosine hydroxylase in hypothalamus by combined autoradiography and immunocytochemistry. Endocrinology 1988;123: 1110–1118.
7 Sar M, Parikh I: Immunohistochemical localization of estrogen receptor in rat brain, pituitary and uterus with monoclonal antibodies. J Steroid Biochem 1986;24:497–503.
8 Munn AR, Sar M, Stumpf WE: Topographic distribution of progestin target cells in hamster brain and pituitary after injection of (3H) R5020. Brain Res 1983;274:1–10.
9 Krieger MS, Morrell JI, Pfaff DW: Autoradiographic localization of estradiol-concentrating cells in the female hamster brain. Neuroendocrinology 1976;22:193–205.
10 Pfaff DW, Schwartz-Giblin S, McCarthy MM, Kow LM: Cellular and molecular mechanisms of female reproductive behaviors; in Physiology of Reproduction, ed 2. New York, Raven Press, 1994, vol 2, pp 150–220.
11 Pfaff DW, Sakuma Y: Deficit in the lordosis reflex of female rats caused by lesions in the ventromedial nucleus of the hypothalamus. J Physiol 1979;288:203–210.
12 Law T, Meagher W: Hypothalamic lesions and sexual behavior in the female rat. Science 1958; 128:1626–1627.
13 Goy RW, Phoenix CH: Hypothalamic regulation of female sexual behavior; establishment of behavioural oestrus in spayed guinea-pigs following hypothalamic lesions. J Reprod Fertil 1963;5:23–40.
14 Kennedy GC: Hypothalamic control of the endocrine and behavioral changes associated with oestrus in the rat. J Physiol 1964;172:383–392.
15 Pfaff DW, Sakuma Y: Facilitation of the lordosis reflex of female rats from the ventromedial nucleus of the hypothalamus. J Physiol 1979; 288:189–202.
16 Delville Y, Blaustein JD: A site for estradiol priming of progesterone-facilitated sexual receptivity in the ventrolateral hypothalamus of female guinea pigs. Brain Res 1991;559:191–199.
17 Rubin BS, Barfield RJ: Progesterone in the ventromedial hypothalamus facilitates estrous behavior in ovariectomized, estrogen-primed rats. Endocrinology 1983;113:797–804.
18 Rubin BS, Barfield RJ: Induction of estrous behavior in ovariectomized rats by sequential replacement of estrogen and progesterone to the ventromedial hypothalamus. Neuroendocrinology 1983;37:218–224.
19 Mathews D, Edwards DA: The ventromedial nucleus of the hypothalamus and hormonal arousal of sexual behaviors in the female rat. Horm Behav 1977;8:40–51.
20 Conrad LC, Pfaff DW: Efferents from medial basal forebrain and hypothalamus in the rat. J Comp Neurol 1976;169:221–262.
21 Saper CB, Swanson LW, Cowan WM: An autoradiographic study of the efferent connections of the lateral hypothalamic area in the rat. J Comp Neurol 1979;183:689–706.
22 Canteras NS, Simerly RB, Swanson LW: Organization of projections from the ventromedial nucleus of the hypothalamus: A *Phaseoulus vulgaris* leucoagglutinin study in the rat. J Comp Neurol 1994;348:41–79.
23 Krieger M, Conrad C, Pfaff D: An autoradiographic study of the efferent connections of the ventromedial nucleus of the hypothalamus. J Comp Neurol 1979;183:785–815.
24 Ricciardi KH, Turcotte JC, De Vries GJ, Blaustein JD: Identification of efferent projections from the steroid receptor-containing area of the ventrolateral hypothalamus in female guinea pigs. J Neuroendocrinol 1996;8:673–685.
25 Shen CL: Efferent projections from the lateral hypothalamus in the guinea pig: An autoradiographic study. Brain Res Bull 1983;11:335–347.
26 Ricciardi KH, Blaustein JD: Projections from ventrolateral hypothalamic neurons containing progestin receptor- and substance P-immunoreactivity to specific forebrain and midbrain areas in female guinea pigs. J Neuroendocrinol 1994;6:135–144.
27 Carstens E, Leah J, Lechner J, Zimmermann M: Demonstration of extensive brainstem projections to medial and lateral thalamus and hypothalamus in the rat. Neuroscience 1990; 35:609–626.
28 Zaborszky L: Afferent connections of the medial basal hypothalamus. Adv Anat Embryol Cell Biol 1982;69:1–107.
29 Delville Y, Blaustein JD: Estrogen receptor-immunoreactive forebrain neurons project to the ventrolateral hypothalamus in female guinea pigs. J Comp Neurol 1993;334:571–589.
30 Cottingham SL, Pfaff DW: Interconnectedness of steroid hormone-binding neurons: Existence and implications; in Current Topics in Neuroendocrinology. Berlin, Springer, 1986, vol 7, pp 223–249.
31 Pfaff D: Patterns of steroid hormone effects on electrical and molecular events in hypothalamic neurons. Molec Neurobiol 1989;3:135–154.
32 De Vries GJ, Gonzales CL, Yahr P: Afferent connections of the sexually dimorphic area of the hypothalamus of male and female gerbils. J Comp Neurol 1988;271:91–105.
33 Blaustein JD, Turcotte JC: Estrogen receptor immunostaining of neuronal cytoplasmic processes as well as cell nuclei in guinea pig brain. Brain Res 1989;495:75–82.
34 Blaustein JD, Lehman MN, Turcotte JC, Greene G: Estrogen receptors in dendrites and axon terminals in the guinea pig hypothalamus. Endocrinology 1992;131:281–290.
35 Paxinos G, Watson C: The Rat Brain in Stereotaxic Coordinates. New York, Academic Press, 1986.
36 Bleier R: The Hypothalamus of the Guinea Pig – A Cytoarchitectonic Atlas. Madison, The University of Wisconsin Press, 1983.
37 Zaborszky L, Leranth C, Makara GB, Palkovits M: Quantitative studies on the supraoptic nucleus in the rat. II. Afferent fiber connections. Exp Brain Res 1975;22:525–540.
38 Nishizuka M, Pfaff DW: Intrinsic synapses in the ventromedial nucleus of the hypothalamus: An ultrastructural study. J Comp Neurol 1989; 286:260–268.
39 Kiss JZ, Palkovits M, Zaborszky L, Tribollet E, Szabo D, Makara GB: Quantitative histological studies on the hypothalamic paraventricular nucleus in rats. II. Number of local and certain afferent terminals. Brain Res 1983;265: 11–20.
40 Blaustein JD, King JC, Toft DO, Turcotte JC: Immunocytochemical localization of estrogen-induced progestin receptors in guinea pig brain. Brain Res 1988;474:1–15.
41 Saper CB, Swanson LW, Cowan WM: The efferent connections of the ventromedial nucleus of the hypothalamus of the rat. J Comp Neurol 1976;169:409–442.
42 Kita H, Oomura Y: An HRP study of the afferent connections to rat medial hypothalamic region. Brain Res Bull 1982;8:53–62.
43 Morrell JI, Pfaff DW: Characterization of estrogen-concentrating hypothalamic neurons by their axonal projections. Science 1982;217: 1273–1276.
44 Ter Horst GT, Luiten GM: *Phaseolus vulgaris* leucoagglutinin tracing of intrahypothalamic connections of the lateral, ventromedial, dorsomedial and paraventricular hypothalamic nuclei in the rat. Brain Res Bull 1987;18:191–203.
45 Gerfen C, Sawchenko P, Carlsen J: The PHA-L anterograde axonal tracing method; in Heimer L, Zaborsky L (eds): Neuroanatomical Tract-Tracing Methods. New York, Plenum Press, 1989, pp 19–47.

46 Gerfen CR, Sawchenko PE: An anterograde neuroanatomical tracing method that shows the detailed morphology of neurons, their axons and terminals: Immunohistochemical localization of an axonally transported plant lectin, *Phaseolus vulgaris* leucoagglutinin. Brain Res 1984;290:219–238.
47 Turcotte JC, Blaustein JD: Immunocytochemical localization of midbrain estrogen receptor- and progestin receptor-containing cells in female guinea pigs. J Comp Neurol 1993;328: 76–87.
48 Warembourg M, Poulain P, Jolivet A: Progesterone receptor-containing neurons in the guinea-pig mediobasal hypothalamus have axonal projections to the medial preoptic area. J Neuroendocrinol 1992;4:273–279.
49 Morrell J, Schwanzel-Fukuda M, Fahrbach S, Pfaff D: Axonal projections and peptide content of steroid hormone concentrating neurons. Peptides 1984;5:226–239.
50 Akesson TR, Simerly RB, Micevych PE: Estrogen-concentrating hypothalamic and limbic neurons project to the medial preoptic nucleus. Brain Res 1988;451:381–385.
51 DonCarlos L, Morrell J: A subset of progesterone target neurons have axonal projections to the midbrain. Brain Res 1990;521:213–220.
52 Aksson TR, Ulibarri C, Truitt S: Divergent axon collaterals originate in the estrogen receptive ventromedial nucleus of hypothalamus in the rat. J Neurobiol 1994;25:406–414.
53 Morrell JI, Corodimas KP, DonCarlos LL, Lisciotto CA: Axonal projections of gonadal steroid receptor-containing neurons. Neuroprotocols 1992;1:4–15.
54 Edwards DA, Pfeifle JK: Hypothalamic and midbrain control of sexual receptivity in the female rat. Physiol Behav 1981;26:1061–1067.
55 Pfeifle JK, Shivers M, Edwards DA: Parasagittal hypothalamic knife cuts and sexual receptivity in the female rat. Physiol Behav 1980;24: 145–150.
56 Sakuma Y, Pfaff DW: Properties of ventromedial hypothalamic neurons with axons to midbrain central gray. Exp Brain Res 1982;46: 292–300.
57 Depaulis A, Keay K, Bandler R: Longitudinal neuronal organization of defensive reactions in the midbrain periaqueductal gray region of the rat. Exp Brain Res 1992;90:307–318.
58 Bandler R, Shipley MT: Columnar organization in the midbrain periaqueductal gray: Modules for emotional expression? Trends Neurosci 1994;17:379–389.
59 Shipley MT, Ennis M, Rizvi TA, Behbehani MM: Topographical specificity of forebrain inputs to the midbrain periaqueductal gray: Evidence for discrete longitudinally organized inputs columns; in Depaulis A, Bandler R (eds): The Midbrain Periaqueductal Gray Matter: Functional, Anatomical, and Neurochemical Organization. New York, Plenum Press, 1991; pp 417–448.
60 Van Bockstaele E, Aston-Jones G, Pieribone VA, Ennis M, Shipley MT: Subregions of the periaqueductal gray topographically innervate the rostral ventral medulla in the rat. J Comp Neurol 1991;309:305–327.
61 Robbins A, Schwartz-Giblin S, Pfaff D: Ascending and descending projections to medullary reticular formation sites which activate deep lumbar back muscles in the rat. Exp Brain Res 1990;80:463–474.
62 Corodimas K, Morrell J: Estradiol-concentrating forebrain and midbrain neurons project directly to the medulla. J Comp Neurol 1990; 291:609–620.
63 Hoshina Y, Takeo T, Nakano K, Sato T, Sakuma Y: Axon-sparing lesion of the preoptic area enhances receptivity and diminishes proceptivity among components of female rat sexual behaviour. Behav Brain Res 1994;61:197–204.
64 Takeo T, Chiba Y, Sakuma Y: Suppression of the lordosis reflex of female rats by efferents of the medial preoptic area. Physiol Behav 1993; 53:831–838.
65 Rodriguez-Sierra JF, Terasawa E: Lesions of the preoptic area facilitate lordosis behavior in male and female guinea pigs. Brain Res Bull 1979;4:513–517.
66 Shimura T, Shimokochi M: Neuronal activity in the medial preoptic area during female copulatory behavior by the rat. Neuroscience 1990; 16:445–450.
67 Yamanouchi K, Arai Y: Forebrain and lower brainstem participation in facilitatory and inhibitory regulation of the display of lordosis in female rats. Physiol Behav 1983;30:155–159.
68 Kondo Y, Koizumi T, Arai Y, Kakeyama M, Yamanouchi K: Functional relationships between mesencephalic central gray and septum in regulating lordosis in female rats – effect of dual lesions. Brain Res Bull 1993;32:635–638.
69 Arendash GW, Gorski RA: Suppression of lordotic responsiveness in the female rat during mesencephalic electrical stimulation. Pharmacol Biochem Behav 1983;19:351–357.